ISSN NO. 2320-5407

Journal homepage: http://www.journalijar.com

INTERNATIONAL JOURNAL OF ADVANCED RESEARCH

RESEARCH ARTICLE

Optical X- Radiation Sensor, and electrical properties of flash evaporated $AgInTe_2$ thin Films

A.M. A. El-Barry*,H.S.Soliman, and S.Y.EL-Soly
Physics Department, Faculty of Education, Ain Shams University, Cairo, Egypt.

Manuscript Info

Manuscript History:

Received: 22 September 2015
Final Accepted: 25 October 2015
Published Online: November 2015

Key words:

Thin film; X-Radiation; thermoelectric power; ac-conductivity

****Corresponding Author***

A.M. A. El-Barry
E-mail:amaelbarry@yahoo.com

Abstract

Thin films of $AgInTe_2$ compound with various thicknesses have been deposited onto both glass and quartz substrates using flash evaporation technique at room temperature. The spectral distribution of both the refractive index (n) and the absorption index (k) and hence the absorption coefficient (α) were studied over a range of wavelength from 200 to 2500 nm .The effect of X-radiation (with different doses ranged from 0 to 12.5 KGy on the optical properties was investigated for dosimetry applications. It was found that both n and k increased as the dose increased and the position of n_{max} was shifted to lower wavelength λ_c. The optical data were analyzed to obtain dielectric constants (ε_∞ and ε_L), where they increased as the value of the dose increased. On the other hand, the absorption edges have been shifted to higher wavelength which was associated with three allowed direct transition as the dose of X-ray radiation increased from 2.5 to 12.5 KGy. Also, the dark electrical resistivity measurements were carried out through a temperature range (298- 423K).An estimation of mean free path (L_0) of charge carriers in $AgInTe_2$ thin films and bulk resistivity, ρ_B was attempted. Measurements of thermoelectric power confirmed that $AgInTe_2$ thin films behave as p-type semiconductors. Finally, the ac conductivity (σ_{ac}) has been investigated in the frequency range (10^2- 10^6 MHz) and temperature range (298 – 407 K). σ_{ac} was found to be proportional to ω^s , where s increased as the temperature increased. Finally; The ac conductivity interpreted by the NSPT model.

Copy Right, IJAR, 2015,. All rights reserved

1-Introudution

The ternary (ABX_2) semiconductors (S.Cs) exhibit a far richer range of physical and chemical properties. These (S.Cs) were discussed in a number of review articles as mentioned before[1]. The broad range of optical band gaps and carrier motilities offered by ternary (ABX_2) semiconductors, as well as their ability to form various solid solutions and to accommodate different dopants, has led to their emergence as technologically significant device materials, including applications in photovoltaic solar cells both as single-crystal materials up to 12% efficient [1,2] and as polycrystalline thin films at least 9.4% efficient, light-emitting diodes [1,3], and in various nonlinear optical devices [1,4]. The previous work [1] deduced that the thin films of $AgInTe_2$ which prepared on quartz substrates by a flash evaporation technique at substrate temperature ~303 K were characterized by a tetragonal structure while the as deposited films have amorphous nature. On annealing at 423 and 573 K (for two hours and under vacuum ~10^{-3} Pa), the films were identified to be single-phase, polycrystalline with a preferred (112) orientation, see Fig.1a. [1.].The optical properties of the films were investigated using spectrophotometric measurements of transmittance and reflectance at normal incidence in the wavelength range (~500–2500 nm). The refractive index (n) and the absorption index (k) of $AgInTe_2$ were determined from the absolute values of the measured transmittance and

reflectance. It was found that both (n) and (k) appeared to depend markedly on the temperature of heat treatment. The dispersion of refractive index in $AgInTe_2$ was analyzed using the concept of the single oscillator model. Within this concept, some dispersion parameters were determined for as deposited and annealed flash evaporated $AgInTe_2$ films at 423 K for 2 h. The calculated values of β indicated that $AgInTe_2$ films belong to ionic class. The ratio of the free carrier concentration of the effective mass (N/m*) were, also determined. The analysis of the absorption coefficient indicated that, this ternary chalcopyrite compound has three allowed direct transitions corresponding to three energies gaps Eg_1, Eg_2 and Eg_3.The crystal field (Δ_{cf}), the spin orbit (Δ_{so}) and the deformation potential (b) were calculated for both as deposited and annealed flash $AgInTe_2$ films at ~ 423 K for 2 h.

In the present work , the effect of X-ray radiation on the optical properties , the dc- conductivity, thermoelectric power and ac-conductivity measurements have been performed , on flash evaporated thin films in the temperature range (298- 423K) and in the frequency range (10^2- 10^6 MHz).

2. Experimental details

The regime of preparation of the ternary compound $AglnTe_2$ in both powder form as well as thin film form was illustrated in detail in the previous work [1]. $AgInTe_2$ films were prepared by flash evaporation technique onto pre-cleaned glass and quartz substrates held at a temperature ~303 K using a high vacuum coating unit (Edwards E 306 A, England). An X-ray diffractometer (Philips X, pert), using Cu radiation operating at 40 kV and 30 mA, was used to investigate the structure. The transmission, T, and reflection, R, spectra were carried out in the wavelength range (~500–2500 nm) and the analysis of the obtained data were carried out as mentioned befor[1]. The electrical resistance, R of planner structure $AgInTe_2$ films of different thickness was measured in a temperature range (~298–423 K), according to two point probe method and using an electrometer with high input impedance (Keithley 617A). The ohmic contacts were made by evaporating gold electrodes. The electrical resistivity, ρ was determined by measuring the film resistance, R using two point probe method for a planner films. In order to study the effect of annealing, $AgInTe_2$ films were heated, in vacuum, at 623 K for two hours. The thermoelectric power was measured using the differential technique with copper electrodes. The films have a dimension ~ 3.5×0.5 cm^2. The electromotive force, ΔE, associated with the temperature gradient along the films was measured using an electrometer (keithly 617). For ac measurements, $AgInTe_2$ films with ~ 503 nm thickness were sandwiched between two evaporated (Au) electrodes. The ac conductivity and some dielectric properties were measured from 50 Hz to 5 MHz frequency range and from 303 to 473K temperature range. A programmable automatic RLC bridge (Hioki 3532 Hitester) was used to measure the impedance Z, the capacitance C and the dissipation factor D.

3. Results and discussion

3.1. The effect of X-ray irradiation on the Structure of $AgInTe_2$ thin films

Fig.1b exhibits the diffraction patterns for the as- deposited and an irradiated $AgInTe_2$ thin films (with 503 nm thickness) with 2.5,6 and 12.5 KGy of X-rays. The patterns indicated that $AgInTe_2$ thin films have amorphous nature. The amorphous structure of the as-deposited films on, substrates kept at room temperature, was expected because the evaporation molecules precipitate randomly on the surface of the substrate and all the following condensed molecules also adhere randomly leading to disordered films. The loss of adequate kinetic energy for the precipitated molecule keeps them unable to orient themselves to produce the chain structure required for the crystalline structure of $AgInTe_2$ thin films .The internal stresses generated in the layers of the films due to the continuous deposition of the hot molecule on the cold predeposited layers increase both the disorder and the degree of randomness which in turn lead to amorphous films whatever their thickness is formed at room temperature [5].

3.2. The effect of X-ray irradiation on the optical properties of $AgInTe_2$ thin films

Since, One of the most accurate methods for determining the energy band structure of semiconductors is that based on investigating the spectral distribution of both the refractive index (n) and the absorption index (k) and hence absorption coefficient (α) . This part deals with new results associated with the optical properties of flashy evaporated $AgInTe_2$ thin films after the radiation with X-ray. Thin films of different thickness (ranging from 208 to 350 nm) were prepared by flash evaporation in vacuum of about 10^{-4} Pa, on optical flat quartz substrates kept at room temperature in similar manner as that exhibited before [1]. Fig.2a represents the spectral dependence of the average values of the absorption index ,(k), for different doses of X-ray irradiation, while Fig.2b represents the average values of the spectral dependence of the refractive index ,(n), on the wavelength. The figures illustrate that

both (n) and (k) increased as the dose increased and the position of n_{max} has shifted to lower wavelength (see the inset of Fig.2b) .Also, the figure illustrates that (**n**) has the same behavior of the as deposited films (dose = 0KGy). The mean refractive index (the average value of the refractive index) attained a peak value at a critical wavelength (λ_c), where its value was shifted towards the shorter wavelength (λ) as the dose increased. The data on the spectral dependence of the refractive index were evaluated according to the single-effective-oscillator model and all the optical data could be described to a very good approximation, by the following equations [1,6-8] .

$$n^2 (h\nu)=1+ [E_0E_d \ / \ (E_0^2 - (h\nu)^2)] \qquad (1\text{-a})$$

$$n^2 = \varepsilon_L - [(e^2N/4\Pi\varepsilon_0 c^2m^*)]\lambda^2 \qquad (1\text{-b})$$

Where ($h\nu$) is the photon energy, E_0 is the oscillator energy, E_d is the oscillator strength or dispersion energy, (N/m*) is the ratio of the carrier concentration to the effective mass, c is the speed of light, and e is the electronic charge.

Plotting $(n^2 - 1)^{-1}$ vs. $(hv)^2$ [see (Fig.3a)] allows one to determine the oscillator parameters by fitting a straight line to the points. The oscillator energy, the dispersion energy, and the high frequency dielectric constant ($\varepsilon\infty$) were determined from the intercept and the slope of the straight lines of the relation between n^2 and λ^2 (see the inset of Fig.3a). The obtained data are listed in Table.1, where E_o decreased while $\mathbf{E_d}$, ε_L and ε_∞ increased as the dose of X-irradiation increased. This behavior may be attributed to the increase in the density of traps caused by the exposure to X-ray, which in turn, increased the disorder [9]. The variation of the dispersion parameters for the irradiated $AgInTe_2$ **thin** films with the dose of X-Ray could be represented by the following empirical relation **:-**

$$\mathbf{E_o = 2.00456 - (0.01523)\, X + (7.45325 \times 10^{-4})\, X^2} \qquad \mathbf{(2\text{-a})}$$

Where x represents the value of the dose of X-ray while the dependence of dispersion energy (E_d) on different doses could be represented by;

$$\mathbf{E_d = 17.68859 - (0.10205)\, X + (0.01124)\, X^2} \qquad \mathbf{(2\text{-b})}$$

The obtained data were analyzed to obtain dielectric constants ε_∞ and ε_L. The calculated results are given in table 1. They increased as the dose increased but they have larger values compared with the as-deposited thin $AgInTe_2$ films. On the other side, the E_g and its related parameters decreased with increasing the dose [see table 2] and that may be due to the increasing of the amorphicity of the materials and this is supported by the increasing of the dispersion parameters E_d, ε_∞ and ε_L, also one can observe that the difference between ε_L and ε_∞ is still presents where ε_L is greater than ε_∞ and the reason of that has been explained before in [9].

The variation of the lattice dielectric constant and the high frequency dielectric constant for our $AgInTe_2$ **thin** films could be represented by the following empirical relations:-

$$\mathbf{\varepsilon_L = 12.29768 + (0.05574)\, X + (0.00192)\, X^2} \qquad \mathbf{(2\text{-c})}$$

$$\mathbf{\varepsilon_\infty = 9.82516 + (0.01575)\, X + (0.0025)\, X^2} \qquad \mathbf{(2\text{-d})}$$

Also, the spectral variation of the absorption coefficient ($\alpha = 4\Pi k/\lambda$) for as deposited and irradiated films are represented in Fig.3b as in the form of (α-α_0) after the correction of background absorption, (α_0). The same figure indicating the reduction of (α) with X-irradiation .The variation of the optical absorption near the fundamental absorption edge has allowed us to determine the optical energy gap as mentioned before [1,10,11].

$$(\alpha-\alpha_0)\, hv = A\ (hv - Eg)^r \qquad (3\text{-a})$$

$$E_{1,2} = -0.5\{\Delta_{So} + \Delta_{CF}\} \pm [(\Delta_{So} + \Delta_{CF})^2 - ((8/3)\, \Delta_{So}\, \Delta_{CF})]^{0.5} \qquad (3\text{-b})$$

$$\Delta_{CF} = 0.5[(E_2+E_1) - \{(E_2+E_1)^2 - 6E_1E_2\}^{0.5}] \qquad (3\text{-c})$$

$$\Delta_{SO} = 0.5[(E_2+E_1) + \{(E_2+E_1)^2 - 6E_1E_2\}^{0.5}] \quad (3\text{-d})$$

$$\Delta_{CF} = (3b/2)(2-c/a) \quad (3\text{-e})$$

All the symbols in the prvious equations from (3-a) to (3-e) have the same meaning as mentioned before[1] .Fig.3b reveals that there is no sharp absorption edge which is a sharply characteristic of glassy state and it is observed that α (ω) decreased with increasing of the dose for X-ray irradiation and the position of the fundamental absorption edge shifted to the higher wavelength. Also we found that the allowed direct transitions are still available, and the absorption edge was shifted to higher photon energy. It is clear that irradiation of $AgInTe_2$ films leaded to excitation of non-bonding electrons into conduction band with their subsequent on localized states. The increase of carriers on localized states will lead to decreasing the transition probabilities into the extended states giving rise to additional absorption and hence reducing of the band gap, termed irradiation doses. The values of the direct energy gaps, the spin orbit splitting and the crystal field are given in table .2. The variation of the energy gaps Eg_1, Eg_2 and Eg_3 also, could be represented by the following empirical relations for the irradiated $AgInTe_2$ thin films:-

$$\mathbf{Eg_1 = 0.93737 - (0.00651)\,X + (7.22097\times10^{-5})\,X^2} \quad \textbf{(4-a)}$$

$$\mathbf{Eg_2 = 1.20472 - (0.0123)X + (3.40463\times10^{-4})X^2} \quad \textbf{(4-b)}$$

$$\mathbf{Eg_3 = 1.65007 - (0.00251)\,X + (1.32408\times10^{-4})\,X^2} \quad \textbf{(4-c)}$$

3.3. Dark electrical resistivity measurements of flash evaporated $AgInTe_2$ thin films

The electrical resistivity measurements could be used to investigate the effect of the film thickness and the effect of the sample temperature on the dark electrical resistivity of $AgInTe_2$ thin films either as deposited or after being annealed at 423K/2h. Fig.4 and the inset of it exhibits the dependence of the resistivity, ρ, for the as- deposited and annealed $AgInTe_2$ films ,respectively, on film thickness at different temperatures (298- 423K). From this figure, it is seen that the resistivity decreased with increasing film thickness in accordance with the results for semiconductor films [12-14].In the lower thickness range the decreasing of film resistivity is much higher than that in the high range. In other words, the thickness dependence of the film resistivity is not linear but is rather exponential. Obviously such a change of resistivity of thin film is a common feature of thickness dependence. Also for the annealed films, the same behavior for the as-deposited $AgInTe_2$ films was obtained for annealed films at 423 K for two hours. This behavior indicates that the electrical resistivity exhibits size effect phenomena in these films, according to Tellier model [13] for effective mean free path, which takes to account surface scattering in addition to bulk scattering. The dependence of the resistivity, ρ, of a film on the thickness, d, can be represented as,

$$\rho = \rho_B \left[1 + \frac{3L_0}{8d(1-\rho)} \right] \quad (5\text{-a})$$

,where ρ_B is the bulk resistivity, L_o is the bulk electron mean free path and P is the secularity parameter .The values of mean free path and bulk resistivity before and after annealing for $AgInTe_2$ thin films are listed in Table.3. It was found that the mean free path for annealed films has smaller values than that calculated for as-deposited films. Also the bulk resistivity decreased with annealing, while the mean free path increased with increasing the temperature, which may be due to decreasing of scattering for the charge carriers, then at certain temperature the mean free path beginning to decrease with increasing of scattering for the charge carriers. On the other hand, the mean free path for the annealed films increased with temperature to reach a value nearly equal to that observed for as deposited $AgInTe_2$ thin films [1].

Dark electrical resistivity ρ of thin films with different thickness ranging from (150-300 nm) was measured in the temperature range from ~ 300 to 423 K to obtain the thermal activation energy and illustrated in Fig.(5). The temperature dependence of the resistivity can be expressed by Arrhenius equation [10-12],

$$\rho_f = \rho_0 \exp(\frac{\Delta E}{K_B T}) \quad \text{(5-b)}$$

,where ΔE is the thermal activation energy , ρ_0 is the pre-exponential resistivity and k_B is the Boltzmann's constant. A plot of log (ρ) vs. (1000/T) yields straight lines from them the thermal activation energy of the films.were determined. Fig.5a shows the dependence of the dark electrical resistivity, for as-deposited $AgInTe_2$ thin films of different thickness, on the temperature. As seen from the figure, there are two distinct linear parts, which correspond to two activation energies ΔE_1 and ΔE_2**.** at T < 350 K and T > 350 K respectively. ΔE_1 corresponds to extrinsic conduction, and ΔE_2 is corresponding to intrinsic conduction, and hence the activation energy is interpreted as a change from extrinsic to intrinsic conduction. The value of the thermal activation energy ΔE_1 is nearly 0.271±0.0007 eV and ΔE_2 is nearly equals to 0.614±0.0009 eV و where the value of $\Delta E_2 \approx$ ½ the value of the onset optical gap which illustrated in [1, 10].The temperature dependence of the resistivity for annealed films is shown in Fig.5b. The values of activation energies ΔE_1 and ΔE_2 decreased after annealing to 0.252±0.0007 eV, and 0.615±0.0005 eV respectively.

3.4 Thermoelectric Power measurements of flash evaporated $AgInTe_2$ thin films.

Since the thermoelectric power is a power tool to provide information about the energetic difference between the relevant transport state and the fermi level ,regardless of the details of the transport mechanisms[12,14],where the Seebeck coefficient(S) directly reveals (i) the conduction type (ii)the energy difference between the fermi level and the transport state. Simultaneously, with the DC measurements, the thermo-electric power and Seebeck coefficient (S) of our $AgInTe_2$ thin films with different thickness (150 – 300 nm), have been measured by differential method with (Cu) electrode.

Fig .6 (a,b) illustrates the temperature dependence of (S) for $AgInTe_2$ thin films before and after annealing at (423 K/2h) in the temperature range (300- 423 K).The values of (S) were found to be positive over the entire temperature range similar to those published before [12,15]. The positive values of (S) indicate p-type conduction [12, 16] of $AgInTe_2$ thin films. Also, the figure exhibits that (S) increased firstly with temperature, which may be related to the crystallization range , after which (S) gradually decreased with temperature**.**

The relation of (S) vs. (1000/T K^{-1}) is illustrated in the inset of Fig.6. The range of temperature at which a maximum in S appeared was recognized as the transition from extrinsic to intrinsic conduction. The decreasing in (S),at higher temperature, may be attributed to the large mobility of the generated electrons associated with intrinsic conduction. The Seebeck Coefficient (S), in the lower temperature range, has been described by the following relationship [12, 17];

$$S = \frac{-k_B}{e}[\frac{\Delta E_u}{k_b T} - \frac{\gamma}{k_b} + 1] \quad \text{(6-a)}$$

Where ΔE_u is the energy difference between the fermi level and the transport state, which inecreased from 0.157 eV for the as deposited films to 0.25 eV for the annealed $AgInTe_2$ thin films. On the other hand, (γ), which is the temperature coefficient, was found to be ≈ 3.39 ± 0.025 eV regardless the heat treatment.

By combining Seebeck and conductivity results, we could determine the carrier density. The hole density (p) could be directly calculated according to the following equation [12, 16];

$$n = 2M^{3/2}[\exp\left(\frac{2k_B - S}{K_B}\right)] \quad \text{(6-b)}$$

Where M = [2π m* k_B T/h^2], h is Planck's constant and m* is the effective mass , which was taken as 0.12 m_0 [1-5]. It has been found that p decreased from ~ 9.06×10^{24} /m^3 to 2.18 $\times10^{23}$ /m^3 for as deposited and from ~ 1.68×10^{25} /m^3 to 2.79 $\times10^{23}$/m^3 for the annealed **$AgInTe_2$** thin films, respectively as the temperature increases from ~ 303 to 473K.

In the intrinsic region, the Seebeck coefficient can be given as [12];

$$S = \left(\frac{-K_B}{e}\right)\left(\frac{c-1}{c+1}\right)\left(\frac{\Delta E}{K_B T} + 2\right) \quad (6\text{-c})$$

Where (c) is the mobility ratio i.e., μ_e/μ_h .The application of the above equations leads to calculating the concentration of charge carrier, p. In addition, the value of (c) could be determined from the slope of the graph of S vs., 1000/T in the intrinsic region. The mean values (c) were found to be 0.996 and 0.998 for as deposited and annealed films respectively, where the change in (c) by annealing could be neglected and take the average value of (c) through the prepared films as (c) $\approx 0.997 \pm 0.001$. This means that (μ_e) is slightly lower than (μ_h) and this difference preserve the sigh of thermoelectric power through the intrinsic region.

3.5. ac electrical conductivity and dielectric properties of flash evaporated $AgInTe_2$ thin films

The total electrical conductivity ,$\sigma_{tot}(\omega)$ of sandwiched $AgInTe_2$ films ,with ~ 503 nm thickness , was measured as a function of both temperature and frequency in the temperature range (303-473 K) and frequency range (50Hz - 5MHz). Hence, the total conductivity is a sum of the two components: dc electrical conductivity (σ_{dc}), which is independent of frequency; and frequency dependent conductivity σ_{ac} (ω), i.e [$\sigma_{tot}(\omega) = \sigma_{dc} + \sigma_{ac}(\omega)$]. In the present part, the ac conductivity of $AgInTe_2$ thin films was investigated in a wide frequency and temperature range rang. It is hoped that this study will give a better understanding of the dielectric properties of $AgInTe_2$ films as well as identifying the dominant conduction mechanism. Fig.7a represents the frequency dependence of the ac conductivity at different temperatures. It can be seen that the ac conductivity can be divided into three regions. The low frequency region, from 50Hz to about 1 KHz, is designated as region (1). Intermediate frequency region, from 1 KHz to 1MHz, is designated as region (2). Region (3) is designated for the high frequency region above 1MHz up to 5MHz. In regions 1and 3, the ac conductivity is frequency independent.. For region (2), the ac conductivity strongly depended on the frequency of the applied electric field. Accordingly this, region (2) was called dispersion region. Regardless the temperature, the ac conductivity tended to increase monotonically with increasing the frequency. Also, in the low frequency region, the applied field was not enough to initiate the hopping conduction. In accordingly the conduction mechanism was attributed to drift of carriers and no extra carriers were created [18-19]. For region (2), in which the conductivity increased with increasing the frequency of the applied field, the ac conductivity obeys a power low of frequency according to the famous equation [16-21];

$$\sigma_{(\omega)} = A\,\omega^s \quad (7\text{-a})$$

Where A is a constant, ω is the angular frequency and s is the frequency exponent factor which is generally less than or equal to unity .Such a trend of dispersion has been ascribed to a relaxation caused by carriers hopping between equilibrium sites. In order to determined the frequency exponent factor s, a plot of $\ln\sigma_{(\omega)}$ vs. $\ln\omega$ was drawn, in the dispersion region, [Fig.7b], for different temperatures. From the slopes , s could be obtained as a function of temperature [see the inset of Fig.7b] . The values of s were found to increase slightly with increasing of temperature. Regarding the values of s and its variation with temperature and following S.R. Elliot [18, 23] the small polaron (S.P) model seemed to be the nearest model related to the obtained results. In the small or molecular polaron, [18, 20] the binding energy, W_P, raised from local bonding changes. Hence the distortions round two sites do not overlap and the activation energy for particle transfer will be independent of the separation of the site [20]. Transport of an electron between degenerate sites having a random distribution .Therefore, generally involve an activation energy, for polaron hopping; $W_H \approx W_p / 2$.The conductivity in the NSPT model is given by the following equation [20] ;

$$\sigma_{ac}(\omega) = c^1 e^2 K_B T \alpha_0^{-1} \left[N(E_f)\right]^2 \omega R_\omega^4 \quad (7\text{-b})$$

Where R_ω is the hopping distance at a particular frequency ω given by

$$R_\omega = (2\alpha_0)^{-1} \ln(1/\omega\tau_0) \quad \text{(7-c)}$$

And the frequency exponent is given by.

$$s = 1 - 4/[\ln(1/\omega\tau_0) - W_H / K_B T] \quad \text{(7-d)}$$

Where W_H increased with temperature from 0.82 at T= 303 K to 1.06 at T = 473 K. If we return to Table .1 where the first optical energy gap , $E_{g1} = 0.94 \pm 0.007$ and by comparing this result with that stated by Elliot [18, 21] where;

$$W_M = E_g - W_1 + W_2 \quad \text{(7-e)}$$

And for bipolaron (simultaneous two electrons hopping between charged defects D^+ and D^-); W_1 is taken to be equal to W_2. So the previous equation will be; $W_M \sim E_g$.

Finally, In this study the dielectric properties of $AgInTe_2$ thin films were investigated. The investigation concerned the effect of frequency of the applied field and temperature on the dielectric properties. Fig.8 shows frequency dependence of the dielectric constant ε_1 while the inset of the figure represents the temperature dependence of it, where the dielectric constant continuously decreased with increasing of the frequency. The variation of ε_1 with frequency can be noticed clearly at higher temperatures. The decreasing of ε_1 with frequency can be attributed to the fact that at low frequencies ε_1 for polar material is due to the contribution of multi-component of polarization, deformational polarization (electronic and ionic polarization) and relaxation polarization (orientation and interfacial polarization). When the frequency is increased the dipoles can be rotated sufficiently rapidly, so that their oscillation will begin to lag behind those of the field. As the frequency is further increased the dipole will be completely unable to follow the field and the orientation polarization stopped, so ε_1 begin to decrease approaching a constant value at high frequencies due to the interfacial or space charge polarization, which is effective in multiphase materials. The inset figure shows the temperature dependence of the dielectric constant ε_1 at different constant values of frequencies for $AgInTe_2$ films. Where ε_1 increased as the temperature increased over the whole investigated range of the frequency. The increasing of ε_1 can be attributed to the fact that the dipoles in polar material can not orient themselves at low temperature. When the temperature is increased the orientation of dipoles is facilitated and this increases the value of orientation polarization, and in turn increases ε_1. [12, 22]

Also, the frequency dependence of the dielectric loss ε_2 of $AgInTe_2$ thin films of thickness 503 nm as a representative example could be clarified by plotting ε_2 against lnω for $AgInTe_2$ film as shown in Fig.9, where ε_2 decreased with increasing of frequency. The decreasing of ε_2 with frequency could be attributed to the facts that at low frequencies, the high value of ε_2 is due to the migration of ions in the material. At moderate frequencies, ε_2 is due to the contribution of ions jump, conduction loss of ions jump, conduction loss of ions migration, and ion polarization loss. At high frequencies, the ion vibrations may be the only source of dielectric loss. The inset of Fig.9 shows the temperature dependence of the dielectric loss ε_2 of $AgInTe_2$ films of thickness 503 nm as a representative example where ε_2 increased with increasing of the temperature. Since the dielectric relaxation studies are important to understand the origin of the dielectric losses in a material, the variation of ε_2 with temperature can be explained according to Steven et al [22,24-25] who divided the relaxation phenomenon into three parts, conduction losses, dipole losses, and vibration losses. At low temperatures values of conduction, losses have minimum value since they are proportional to (σ/ω), as the temperature increases σ increases and so the conduction losses increases.

Finally Fig.10a exhibits the variation of the barrier height with temperature. From this figure it is seen that, as the temperature increases the maximum barrier height increases until the transformation (crystallization) temperature, after this range of temperature W_H return to increase gradually with temperature and this may be due to the crystallization. Also, Fig.10b shows the variation of the relaxation time with temperature, where it decreased as the temperature increased until nearly the crystallization range. After this range, the change in the relaxation time could be negligible where τ decreased from 6.405×10^{-11} to 1.054×10^{-11} sec ,while Fig.10c illustrates the variation of polaron radius r_{op} with temperature.

Conclusion

The optical properties of flash evaporated $AgInTe_2$ thin Films were investigated before and after exposure to X-radiation with different doses (from 2.5 to 12.5 KGy) to explore the possibility of their use in dosimetry applications. The analysis of the optical data indicated the predominance of three direct allowed transitions decreased in their values by exposure to X-radiation. The dc measurement supported the presence of two activation energies ΔE_1 and ΔE_2 corresponding to extrinsic and intrinsic conduction respectively, and the thermoelectric power measurement illustrated p-type conduction of the investigated $AgInTe_2$ thin Films .Finally the ac conductivity , in the temperature range (303-473 K) and frequency range (50Hz - 5MHz) obeyed a power law of frequency and the non-overlapping of small polaron (NSPT) seemed to be the nearest model related to the obtained results in the intermediate frequency region from 1KHz to 1MHz.

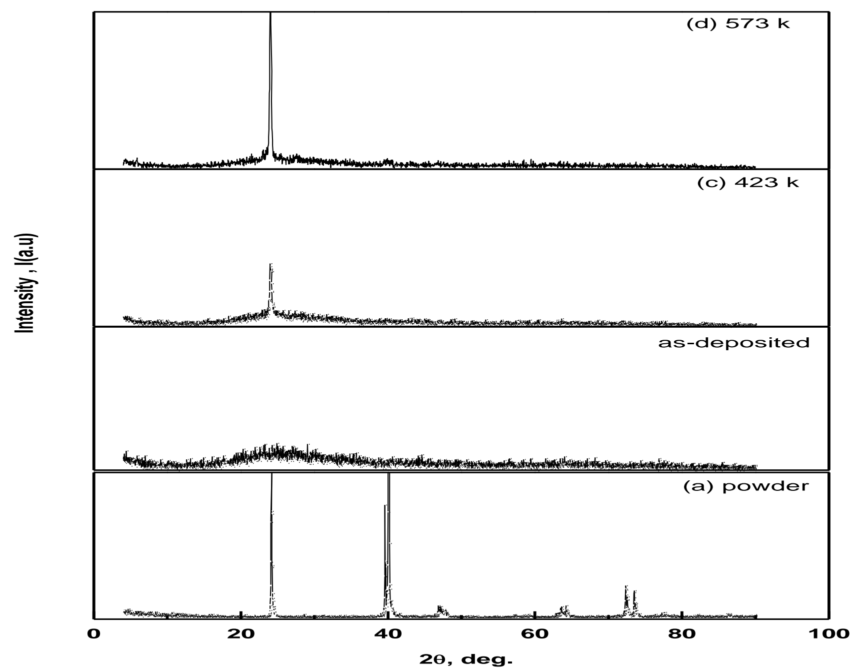

Fig.1a: X-ray diffraction patterns for, (a)a powder of $AgInTe_2$ compound ,(b) as deposited $AgInTe_2$ thin film (503 nm) ; (c) an annealed $AgInTe_2$ thin film (503 nm) at 423K/2h and (d) an annealed $AgInTe_2$ thin film (503 nm)at 523K/2h $AgInTe_2$ [ref.1]

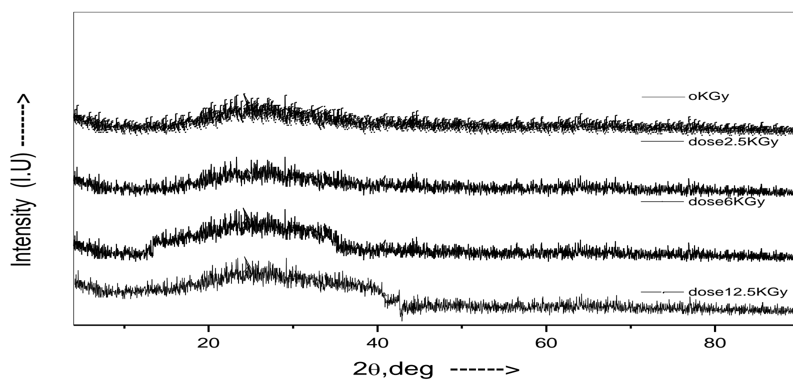

Fig.1b: X-ray diffraction patterns for as deposited and an irradiated $AgInTe_2$ thin films (503 nm thickness), with 2.5,6 and 12.5 KGy of X-radiation

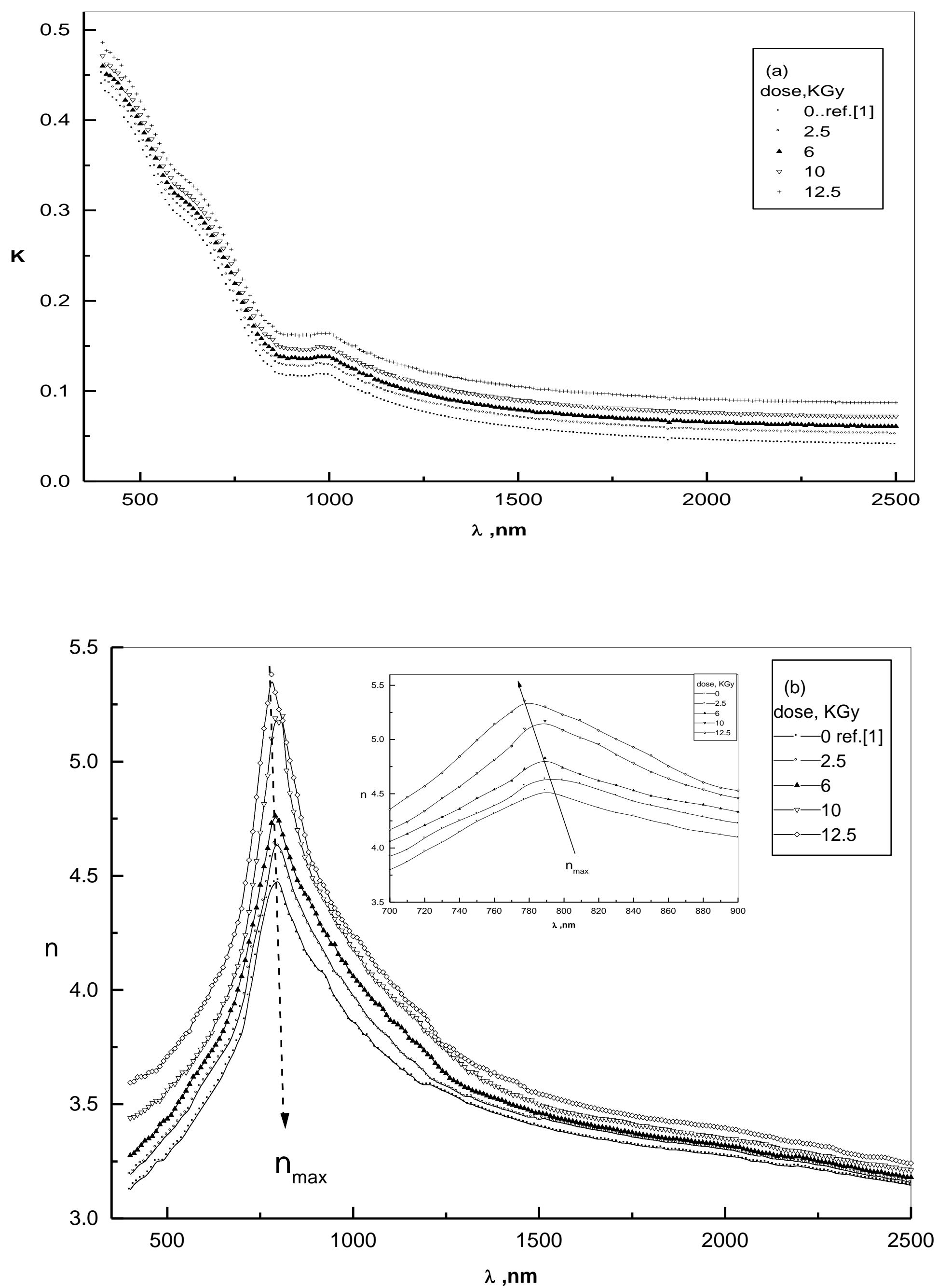

Fig.2: a)The absorption curves of k (λ) for $AgInTe_2$ thin film (503 nm), exposed to different doses of X-radiation, **b**): The dispersion curves of n (λ) for $AgInTe_2$ thin film (503 nm), exposed to different doses of X-radiation; the inset figure represents n vs, λ.

Fig.3a

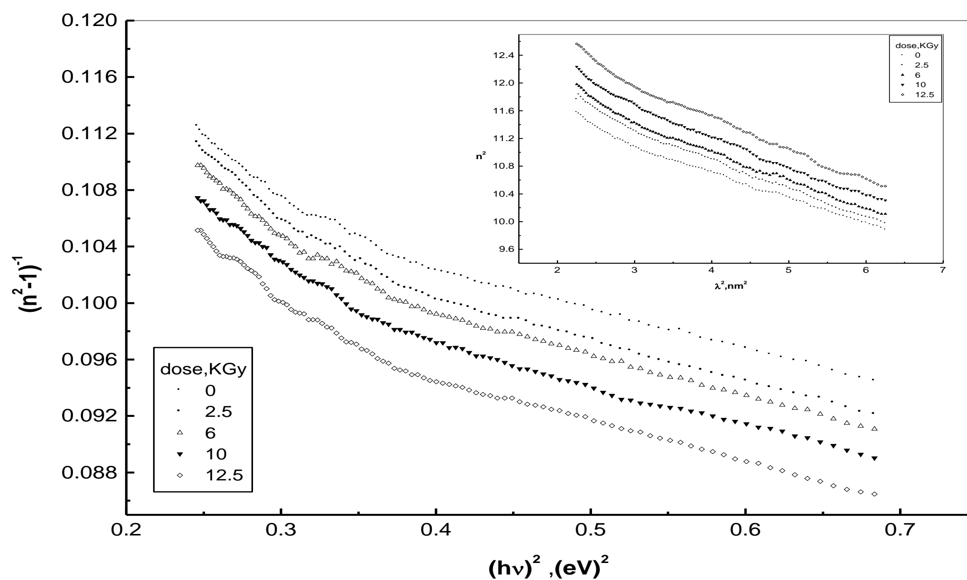

Fig.3a: 1/ (n^2-1) vs. $(h\nu)^2$; the inset figure : n^2 vs. λ^2 for $AgInTe_2$ thin film (503 nm) exposed to different doses of X-radiation .

Fig.3b

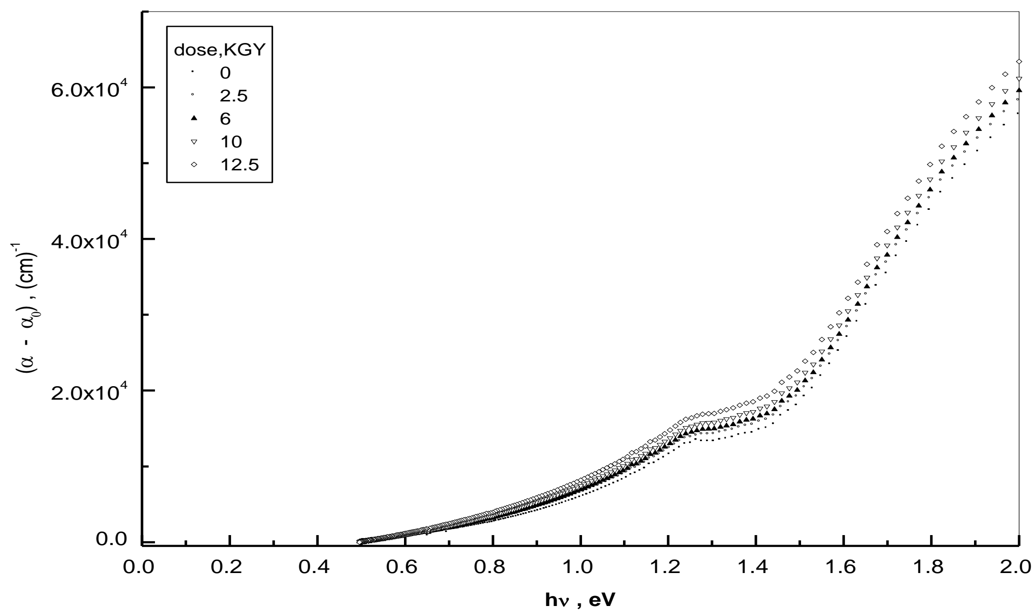

Fig.3b: $(\alpha-\alpha_0)$ vs. $h\nu$ for $AgInTe_2$ thin film (503 nm), exposed to different doses of X-radiation.

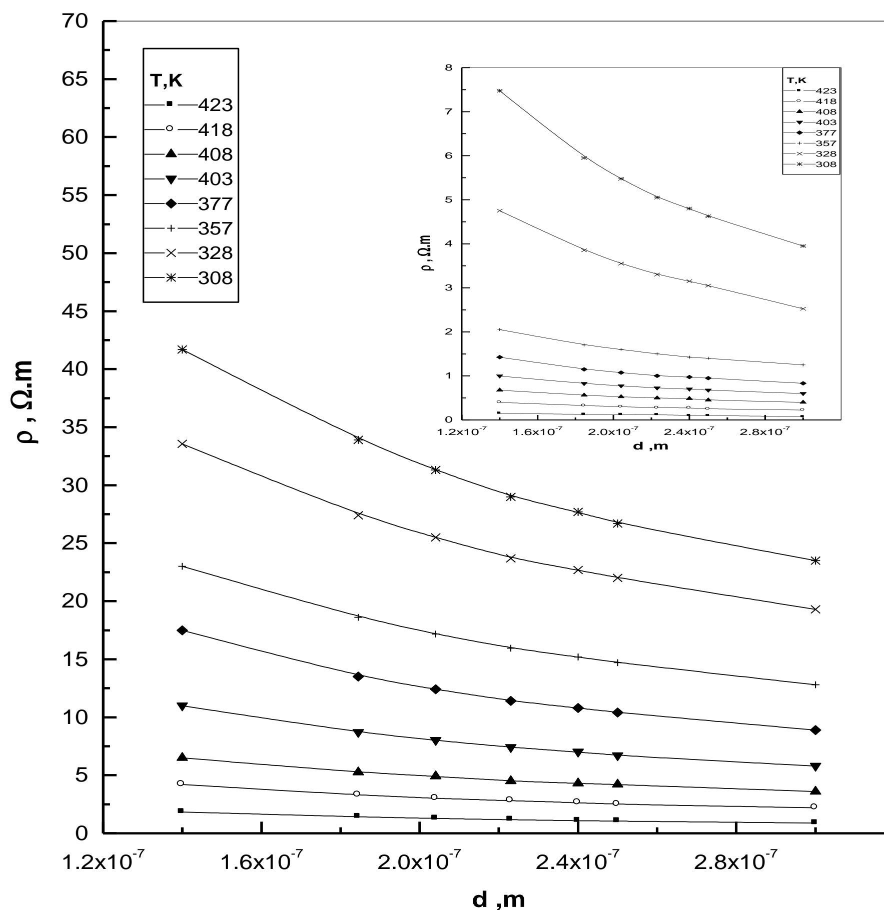

Fig.4: The thickness dependence of the dark electrical resistivity for the as deposited $AgInTe_2$ thin films; the inset figures: ρ vs. d. for an annealed $AgInTe_2$ thin film at 423K/2h.

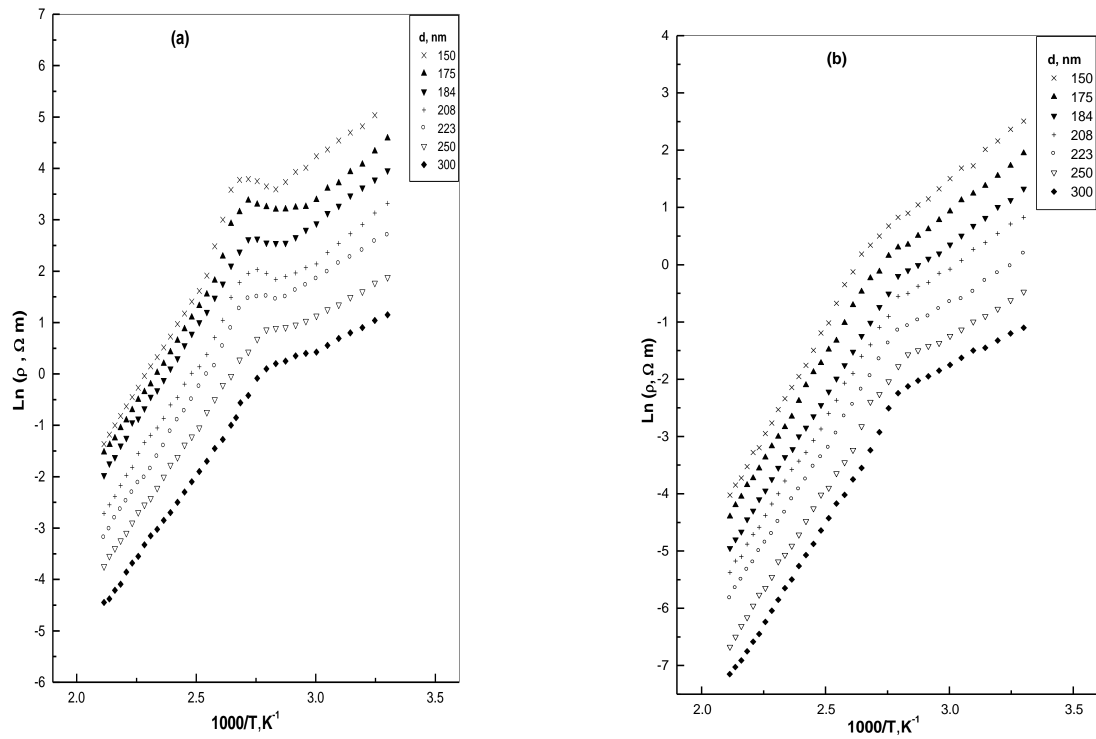

Fig.5: The dark electrical resistivity, ρ, vs. 1000/T for as-deposited $AgInTe_2$ thin films and annealed films at 623K/2h

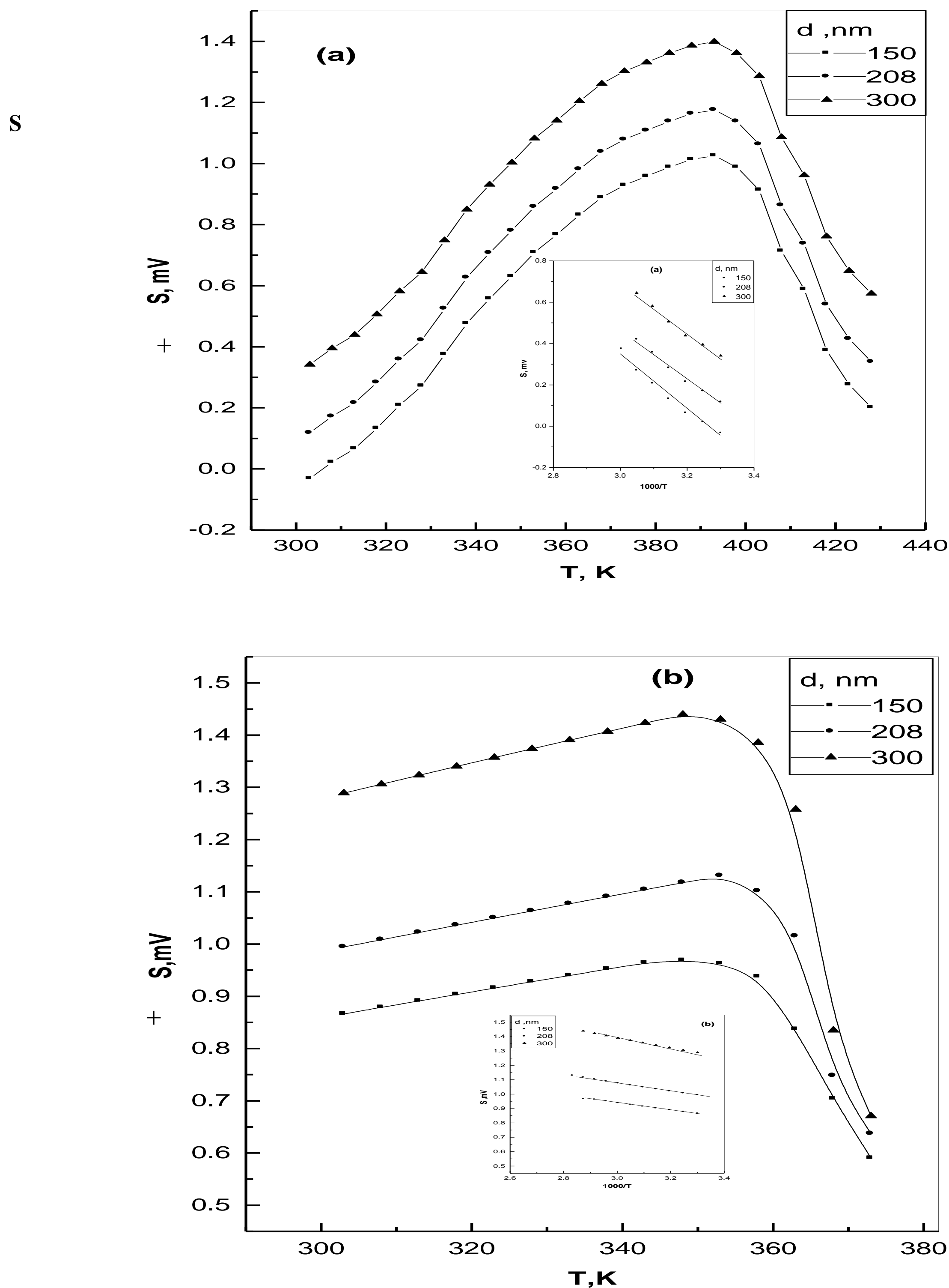

Fig.6: Variation of Seebeck coefficient, S, with T for ;a) as deposited and b) annealed $AgInTe_2$ thin films at 623 K/2h (the inset figure: represents S vs. 1000/T.

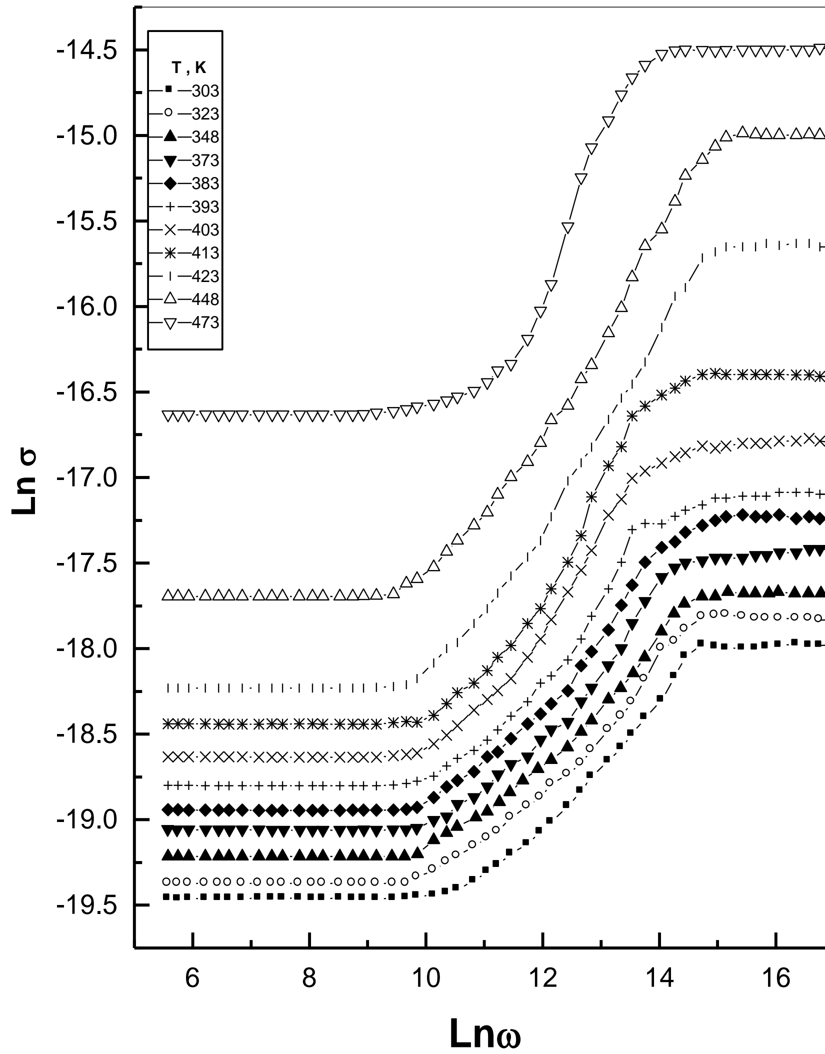

Fig.7a: Frequency dependence of ln ($\sigma_{(tot)}$) at different temperatures for $AgInTe_2$ thin films (503 nm)

.

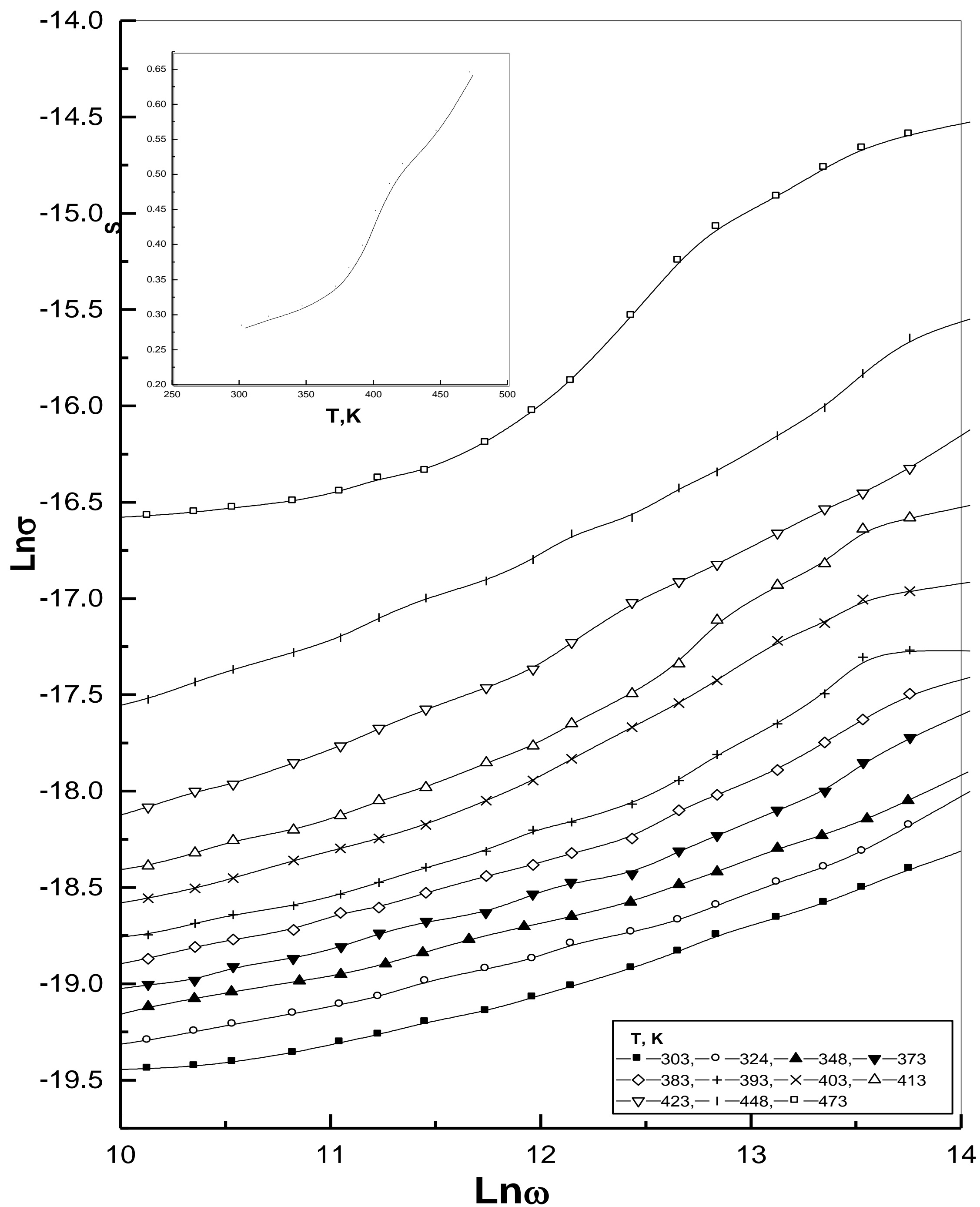

Fig.7b: frequency dependence of ac conductivity for $AgInTe_2$ thin films at different temperature in the intermediate region.

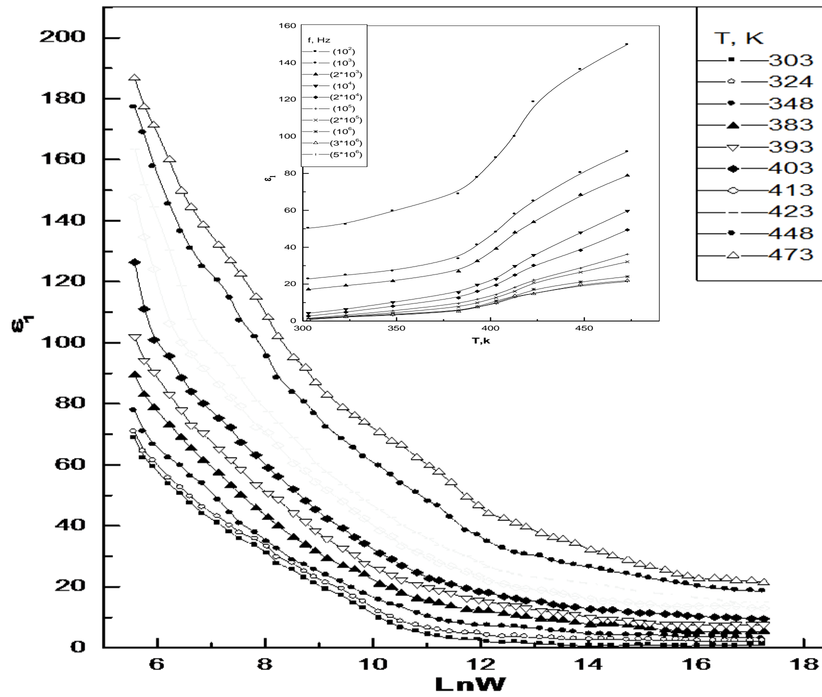

Fig.8: The variation of ε_1 with. ln (ω) ;(the inset figure represents The variation of ε_1 with. T, for $AgInTe_2$ thin films (503 nm)

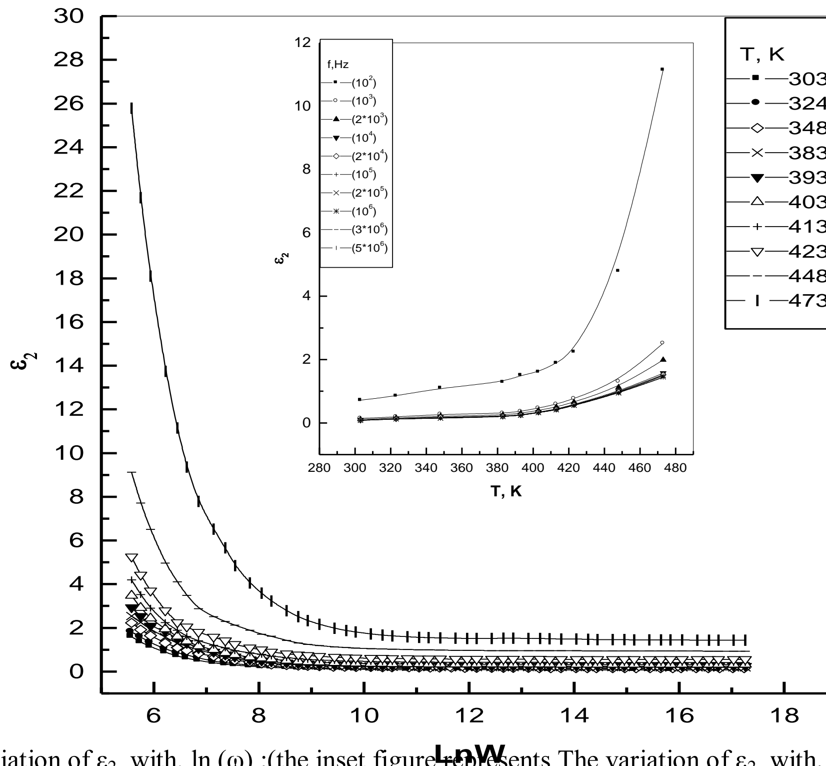

Fig.9: The variation of ε_2 with. ln (ω) ;(the inset figure represents The variation of ε_2 with. T, for $AgInTe_2$ thin films (503 nm)

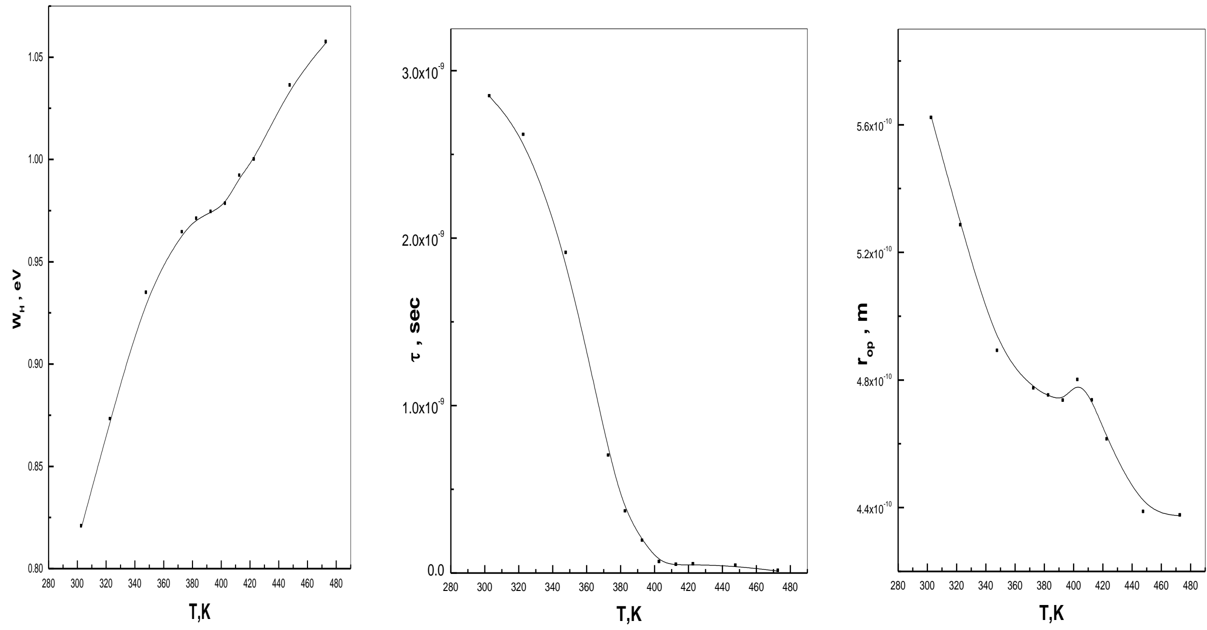

Fig.10:The variation of w_H , τ and r_{op} with temperature for $AgInTe_2$ thin films (503 nm)

Table.1. Some of the dispersion parameters of X-ray irradiated $AgInTe_2$ thin films with different doses 2.5, 6, 10, 12.5 KGy .

Dose, KGy	E_o ,eV	E_d ,eV	ε_∞	ε_L
0[Ref:1]	2.016	17.748	9.804	12.234
2.5	1.949	17.377	9.914	12.567
6	1.948	17.558	10.011	12.668
10	1.935	17.798	10.196	12.982
12.5	1.924	18.153	10.435	13.34

Table.2: The variation of the direct energy gaps, spin orbit splitting and crystal field before and after irradiation with different doses of X-radiation.

Dose, KGy	Eg_1	Eg_2	Eg_3	Δ_{So}	Δ_{CF}
0[Ref:1]	0.94	1.208	1.65	0.51±0.007	-0.34±0.003
2.5	0.918	1.17	1.645	0.54±0.009	-0.32±0.007
6	0.8985	1.145	1.639	0.56±0.009	-0.32±0.001
10	0.8868	1.119	1.639	0.59±0.003	-0.3±0.005
12.5	0.8633	1.1019	1.639	0.61±0.002	-0.31±0.004
Average	0.9±0.001	1.14±0.009	1.64±0.002	0.56±0.008	-0.32±0.002

Table.3. Values of the bulk resistivity, ρ_B, and the mean free path, L_o, for as-deposited and annealed thin films of $AgInTe_2$.

As-deposited films			Annealed films at 423K		
T(K)	ρ_B	$L_o \times 10^{-6}$	T(K)	ρ_B	$L_o \times 10^{-6}$
423	0.24642	2.737	423	0.02618	1.8597
418	0.50317	2.80114	418	0.07279	1.6872
408	0.68235	2.9466	408	0.13928	1.35314
403	1.01281	3.594	403	0.23538	1.17712
377	1.27055	4.7255	377	0.46297	0.88377
357	4.00958	1.7768	357	0.48447	1.156
328	6.5276	1.552	328	0.73497	2.06423
308	9.41939	1.3578	308	0.93683	2.61825

References

1- M.M. El-Nahass, A.M.A. El-Barry , A.A. Farag, and S.Y. El-Soly,Eur. Phys. J. Appl. Phys. **35** (2006) 75

2-S.Wagner,J.L.Shay,P.Migliorato,and H.M.Kasper,Appl . phys.lett.25(1974)434.

3-A.El-Korashy,M.A.EL-Rahim,H.EL-Zahed,Thin Solid Films ,338(1999)207

4- J.E.Jaffe and Alex Zunger ,Phys.Rev.B,28 (100) (1983)5822
.
6- S.H.Wempl, M.DIdominico ,Phys.Rev.,B.3(1971) 1338.

7- S.H.Wempl.Phys.Rev.,B,7(1973)3567.

8-M.M.EL-Nahass,A.A.Atta,M.M.Abd El-Reheem ,and A.M.Hassanine,J.Alloys and Comp.585(2014)1.

9-A.Arshak,S.Zleetni and K.Arshak ,Sensors 2(2002)174.

10- H.Karaagac and M.Parlak,Cryst .Res.Tech.44(4)(2009)440

11- Amarjith Singh ,R.K.Bedi,Thin Solid Films (398- 399)(2001) 427

12-H.S.Soliman ,A.M.A.EL-Barry, N.Kasefan. and M.M.EL-Nahass ,Eur.Phy.J.Applied Physics 37(2007)1

13- C.R.Tellier ,Thin Solid Films 51(1978)311

14- H.S.Soliman ,M.M.Sad Eldin,K.Sawaby and Eledenglaway, Canadin J of pure and applied sciences, 9(1)(2015) 3247.

15- H.S.Soliman, M.M.EL-Nahass,A.M.Farid,A.A.M.Farag and A.A.EL-Shazly,Eur.phys.j.ap.21(2003)187

16- A.M.A.EL-Barry and H.E.Atyia ,Chalcogenide letter ,3,5(2006)41.

17- A.K.Jonscher,Thin Solid Films 36(1976)1

18- S.R.Elliot,Adv.phys.36(1987)135.

19- A.M.A.EL-Barry,H.E.Atyia,Physica B,368(2005)1

20-Aswini Ghoh ,Physical Rev.B 42 (1990) 5665

21-S.R.Elliot,Phil.Mag.36(1977)1291

22- M.A.M.Seyam ,Appl.Sur.sci.181(2001)128

23- S.R.Elliott,Physics of amorphous materials,(John wiley & Sons Inc.) New York,1983

24- J.M.Stevels(The Elctrical properties of glasses)Spring ,Berline(1957)P.350

25-M.M.EL-Nahass,A.M.A.EL-Barry,and S.Abd el Rahman, phys.Stat.Sol.(a)203,No.2(2006)317